

Submitted to: Biophysical Journal, Jan. 05, 2004

Physics of RecA-mediated homologous recognition

Kevin Klapstein,¹ Tom Chou,¹ and Robijn Bruinsma²

¹*Dept. of Biomathematics, UCLA, Los Angeles, CA 90095-1766*

²*Dept. of Physics, UCLA, Los Angeles, CA 90095-1547*

Most proteins involved in processing DNA accomplish their activities as a monomer or as a component of a multimer containing a relatively small number of other elements. They generally act locally, binding to one or a few small regions of the DNA substrate. Striking exceptions are the *E. coli* protein RecA and its homologues in other species, whose activities are associated with homologous DNA recombination. The active form of RecA in DNA recombination is a stiff nucleoprotein filament formed by RecA and DNA, within which the DNA is extended by 50%. Invoking physical and geometrical ideas, we show that the filamentary organization greatly enhances the rate of homologous recognition while preventing the formation of topological traps originating from multi-site recognition.

Keywords: Homologous alignment, RecA, recombination

INTRODUCTION

RecA is a 38kD *E. coli* protein which plays a key role both in DNA repair and in the exchange of genetic material by promoting DNA strand exchange. RecA or a RecA homologue has been found in every species in which it has been sought [Roca & Cox 1997]. RecA mediated strand exchange is important in maintenance of the genome and essential for sexual reproduction. To facilitate strand exchange, RecA polymerizes onto DNA to form a right-handed helical filament with a diameter of $\sim 10\text{nm}$ [Heuser & Griffith 1989] and a repeat length of 6 monomers per helical turn [Yu & Egelman 1992]. Filaments form on both single- and double-stranded DNA (ssDNA and dsDNA) molecules. One form of the filament is the extended filament, formed with an ATP cofactor [Heuser & Griffith 1989, Yu & Egelman 1992]. Extended filaments are very stiff. The persistence length of the extended filaments formed with ssDNA is $\xi_{\text{ssDNA-RecA}} \simeq 860\text{nm}$ [Hegner *et al.* 1999], about 16 times that of dsDNA. The DNA within the extended filament is stretched by 50% relative to B-form DNA.

Many different proteins with diverse functions act on DNA. Of these, RecA is rare in that it forms stable protein *filaments* to accomplish its activity. Stretching the DNA within the filament by 50% is energetically expensive, requiring about $\frac{2}{3}k_B T$ per base pair for dsDNA. This seems to present an *obstacle* to RecA activity by complicating the process of aligning regions of homology between the two substrate DNA molecules. Figure 1 shows how stretching one DNA molecule relative to the other makes it impossible for the homologous regions of the two DNA substrates to stay “in register” with each other. If the DNA molecules are homologously aligned at one base(pair), the neighboring base(pair) is “out of register” by the difference in base(pair) spacing between the stretched and unstretched DNA

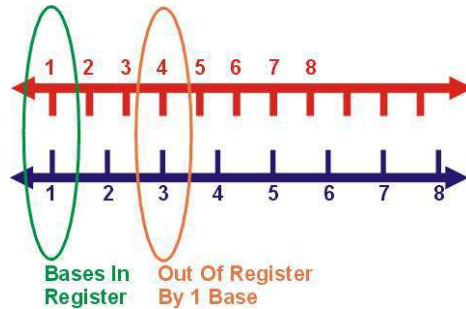


FIG. 1: Unequal spacing between base pairs obstructs homologous alignment. Spacing between consecutive bases on the bottom strand is 50% larger than on the top strand, as for RecA coated DNA. The DNA molecules are homologously aligned at the bases labeled 1. By base 3 on the stretched molecule they are out of register by an entire base.

factor of 50%. Starting from a homologously aligned base(pair), the next to neighboring base along the stretched molecule is already out of register by an entire base.

Other DNA processing proteins, including those associated with DNA recombination and repair, function without needing a filamentous structure, yet RecA and its homologues have preserved the fil-

in species as diverse as *E. coli* and *H. sapiens*. This strongly suggests that it is of value to the system and necessary or at least advantageous in one or more of RecA's activities. The aim of this paper is to use basic physical considerations to understand the role of RecA filaments in RecA function.

FACILITATING INITIAL HOMOLOGOUS ALIGNMENT

Incompatible Inter-Base Spacings

Homology recognition requires identification of many consecutive base pairs as complementary and cannot be accomplished by identifying only a single pair of complementary bases, yet the length of the region which can be simultaneously compared is limited to a single base by the stretching of the DNA within the filament. Surprisingly, we have found that stretching the DNA within the filament does not impede but rather *accelerates* the initial alignment of the homologous regions of the DNA substrates. To see how, consider two B-form DNA molecules having a region of homology. Denote the spacing between consecutive base pairs of B-form DNA by a_0 . If these molecules are parallel then for some position of the one molecule relative to the other the homologous regions will be aligned. As shown in figure 2A, every base pair throughout the region of homology is then homologously aligned. Figure 2B shows the effect of displacing one of the molecules a distance a_0 relative to the other. Now, *none* of the homologous base pairs are aligned. When two DNA molecules have identical spacing between consecutive bases, either *all* bases in the region of homology are aligned or *none* of them are.

Now consider the case when one of the molecules is stretched. The spacing between consecutive base pairs is ηa_0 where the stretching factor $\eta > 1$, as shown with $\eta = \frac{3}{2}$ in figures 2C and 2D. This has two effects on the homologous alignment. First, a base aligned with its homologous counterpart on the other molecule will form the *only* homologously aligned pair. The homologous alignment is lost almost immediately as the two molecules get out of register. When one of the molecules is shifted relative to the other by a distance a_0 , however, a homologous alignment is preserved. The base pair originally homologously aligned is now out of alignment, but two nearby bases have moved into homologous alignment. The behavior is analogous to the operation of a Vernier scale or a slide rule. Alignment is now achieved at only one base pair at a time, but it is far more robust with respect to the relative longitudinal position of the molecules than when η is the same for both molecules.

We define two substrates, \mathcal{D} and \mathcal{R} . \mathcal{D} is a very long B-form dsDNA molecule containing a specific sequence Aa of length J base pairs. \mathcal{R} is a RecA coated ssDNA molecule J bases long and consisting entirely of the sequence A . We first ask what steps

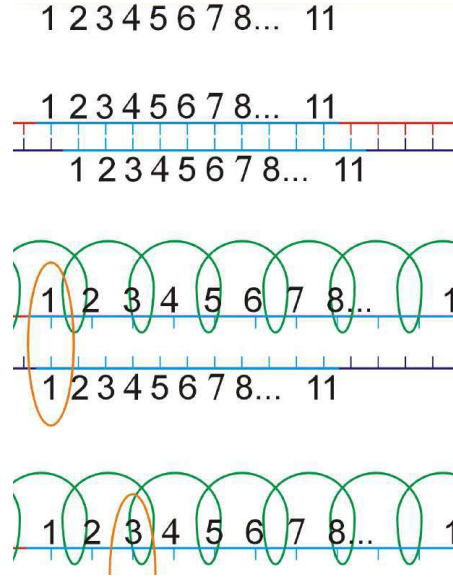


FIG. 2: Alignment between ssDNA molecules. The molecules are homologous in the blue region. (A) Bases are a distance a_0 apart in both molecules. All homologous bases are aligned and in register. (B) The bottom strand has been moved to the right a distance a_0 . Now *none* of the bases are aligned. (C) The upper molecule is coated with RecA. Bases are spaced $3a_0/2$ apart. Although the first base in the region of homology is aligned (orange circle), all others are out-of-register. (D) Moving the bottom strand to the right a distance a_0 does not destroy the alignment, but merely moves its location to the third base in the region of homology (orange circle). All other bases remain out of register.

aligning the J base pair long region of homology between these substrates.

The first contact between the substrates will be as a result of diffusion, and will occur at a point as shown in figure 3A. It has been noted in the literature that there is a weak, non-specific (electrostatic) attraction between the substrates [Karlin & Brocchieri 1996]. This exerts a torque on the substrates, pulling them towards a loose, non-specific parallel alignment as shown in figure 3B.

Recognizing a homologous alignment at any point now involves moving a short *invading segment* of \mathcal{D} into the *interior position* within the RecA filament of \mathcal{R} through the groove in the RecA helix, as shown in figure 3C. To keep the invading segment in register with the DNA of \mathcal{R} requires that the invading segment be stretched by the stretching factor η simultaneously with its entry into the filament. Although this requires significant energy, the process as a whole could remain energetically neutral if the binding energy of the invading segment within the filament is of the same magnitude as the energy required to stretch the invading segment. The movement of the invading segment to the interior position would then be readily accessible to thermal fluctuations and easily reversible. Correct homolo-

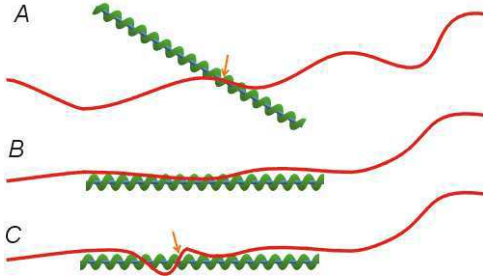


FIG. 3: Red curve, dsDNA molecule (\mathcal{D}); blue line, ssDNA, green helix, RecA filament (\mathcal{R}). (A) Contact at a point (orange arrow). An attractive interaction between \mathcal{D} and \mathcal{R} exerts a torque around this point. (B) The non-specific parallel orientation produced by the torque in A. (C) An invading segment of \mathcal{D} enters the RecA filament of \mathcal{R} through the filament groove (orange arrow).

in the interior position by the formation of hybrid base pairs, which would facilitate the movement of more of \mathcal{D} into the filament and further extension of the region of hybrid DNA. In the absence of homologous alignment, this stabilization could not occur and thermal fluctuations would remove the invading strand from the interior position. In this way large sections of \mathcal{D} and \mathcal{R} can be quickly examined for homologous alignment by thermally driven invasions of different regions of \mathcal{D} at different points along \mathcal{R} , without the need for any relative diffusion of \mathcal{D} and \mathcal{R} in the longitudinal direction.

In a one-dimensional search, a simple model would be to wind a segment of \mathcal{D} non-specifically into the filament and searches for homology by sliding longitudinally within the filament. This is appealing because it avoids repeatedly winding invading segments in and out of the filament, but it has many problems. These include the fact that the experimental evidence excludes significant sliding during the search process [Adzuma 1998], consistent with the observation that the longitudinal sliding of such large molecules would be very slow and inefficient. This would also create a “trap” in which DNA heterologous to the DNA in \mathcal{R} acts as a suicide substrate, hindering the filament’s ability to

blocks the entry of homologous DNA. This poisoning of the reaction does not happen *in vitro* and would be lethal *in vivo*. For these and other reasons, we reject this model.

Target Size Enhancement and Kinetic Perfection

When \mathcal{D} and \mathcal{R} are parallel, movement of invading segments between the interior and exterior positions can be very rapid, allowing the entire parallel length of \mathcal{D} and \mathcal{R} to be efficiently examined for homologous alignment. If there exists a point of alignment, it will be found and the alignment extended throughout the entire homology. This reduces the problem to a question of how likely it is that a random point of initial contact will result in a parallel orientation which has a point of homologous alignment. Stretching of the DNA by RecA plays a crucial role by enhancing this likelihood.

Define the *target size* σ for homologous alignment as the range of longitudinal positions of one DNA molecule relative to another which results in the homologous alignment of at least one base pair. For two B-form DNA molecules, this requires great precision. The molecules must lie within $\pm a_0/2$ of an exact alignment, so the target size is $\sigma = a_0$. If they do lie in this range then *all* the bases are aligned, but this is *not* desirable. Later, we show that an extended region of homologous alignment poses serious problems and is undesirable.

This contrasts with the situation between \mathcal{D} and \mathcal{R} . When \mathcal{R} is stretched by a factor $\eta_{\mathcal{R}}$ the target size for a region of homology J base pairs long is found in Appendix A to be

$$\sigma = [(J - 1)(\eta_{\mathcal{R}} - 1) + 1] a_0 \quad (1)$$

For two unstretched DNA molecules, $\eta_{\mathcal{R}} = 1$ and equation 1 gives the expected result

$$\sigma = a_0 = 0.34\text{nm} \quad (2)$$

but using the known RecA value of $\eta_{\mathcal{R}} = 3/2$ gives $\sigma = (J + 1)a_0/2$, which scales linearly with the homology length. A modest 200 base homology gives

$$\sigma \simeq 100a_0 = 34\text{nm} \quad (3)$$

This huge target size, a 100 fold increase relative to two unstretched DNA molecules, offers an enormous advantage to the homology recognition process. It is achieved only because of the stretching of the DNA within the RecA filament.

The initial point of contact between \mathcal{D} and \mathcal{R} completely determines their relative position when parallel (figures 3A and B). Imagine holding this point fixed on \mathcal{D} while changing it on the \mathcal{R} . Displacing the initial point of contact on \mathcal{D} by a distance d will change the relative position of \mathcal{D} and \mathcal{R} in the parallel orientation by a distance d . This

means that to achieve a homologous alignment the initial contact must occur within a region of length σ .

Knowing the target size allows us to estimate the reaction rate. In the absence of sliding [Adzuma 1998] the reaction rate cannot exceed the diffusion limit, so the maximum “on rate” for the reaction is the Debye-Smoluchowski rate. We approximate the cylindrical target of length σ by a spherical target of radius $\sigma/2$. We also estimate the diffusion constant of \mathcal{R} , which is a cylinder of length ℓ , by the diffusion constant for a sphere with a radius of $\ell/2$. With these approximations we find

$$k_a \simeq \frac{2k_B T}{3\eta} \left(1 - \frac{1}{\eta_{\mathcal{R}}}\right). \quad (4)$$

This result is independent of the length of the homology, the number of base pairs in the region of homology, and the spacing between consecutive base(pair)s in unstretched B form DNA. It depends only on the temperature T , on η , the viscosity of the solution, and on the stretching factor $\eta_{\mathcal{R}}$. The stretching factor for DNA within the RecA filament is $\eta_{\mathcal{R}} = \frac{3}{2}$, and $\eta \simeq 10^{-3}$ poiseuille at 20°C, so we have $k_a \simeq 5.3 \times 10^8 \text{ Mol}^{-1} \text{ sec}^{-1}$.

PREVENTING MULTIPLE HOMOLOGOUS ALIGNMENTS

Topological Trapping

If homologous strand exchange between two substrates is initiated at two or more separate points it will result in a problematic *topological trapping* of the reaction. To extend a region of hybrid DNA, at least one strand of the external dsDNA must wind into the RecA filament [Honigberg & Radding 1998]. If exchange between the substrates is initiated at two separate points, this motion produces compensating *counter-turns* of the dsDNA around the outside of the filament, as shown in figure 4. Extending the hybrid DNA increases the number of counter turns while decreasing the length of dsDNA which forms them, which rapidly decreases the radius of the counter-turns. This makes them very energetically expensive to produce, which eventually stops extension of the hybrid DNA.

Topological trapping can occur only if homologous strand exchange is able to begin at two points. If initiation of homologous strand exchange between the substrates at one point somehow prevents the initiation of homologous strand exchange at any other point along the same two substrates, topological trapping will never occur. To exploit this fact, the strand exchange machinery must impart to the *entire* length of the homology the information that homologous strand exchange has been initiated between them. The problem thus becomes finding a means of communicating over large distances with the fact that homologous strand exchange

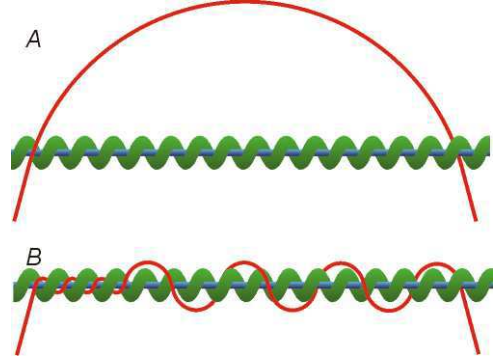


FIG. 4: Topological trapping resulting from initiation of strand exchange at two separate points. Red curve = dsDNA molecule (\mathcal{D}); blue line = ssDNA, green helix = RecA filament (\mathcal{R}). (A) Homologous alignment at alignment regions 1 (left) and 2 (right). These are shown only at their initial point of closest approach but may be of arbitrary length, *e.g.*, region 1 may extend far to the left of what is shown. (B) Extending alignment region 1 to the right requires that \mathcal{D} be “wound into” the filament of \mathcal{R} . This entails rotation of \mathcal{D} and \mathcal{R} , forming “counter turns” of \mathcal{D} around \mathcal{R} . Because \mathcal{D} is fixed relative to \mathcal{R} at region 2, the counter turns are “trapped” between regions 1 and 2.

exchange process should be initiated.

We propose that a key function of the extended filament structure is to prevent topological trapping. Both the stiffness of the filament and the stretching of the DNA within it are essential to accomplishing this. Here, we give a qualitative explanation of how this works. A more detailed treatment appears in Appendix B.

Consider homologous exchange between \mathcal{D} and \mathcal{R} which has extended to encompass a segment of the substrates which we call the *first region*. Symmetry makes it sufficient to consider only the sections of the substrates to one side of the first region. Number the base(pair)s in ascending order to the right, beginning with the right most base(pair) in the first region. If the second contact is at base N on \mathcal{D} , it will be homologously aligned only if it at base pair N on \mathcal{R} . Formation of a *second region* produces a *double hit loop*, half of which is composed of ssDNA from \mathcal{D} and half of which is composed of ssDNA from \mathcal{R} . The

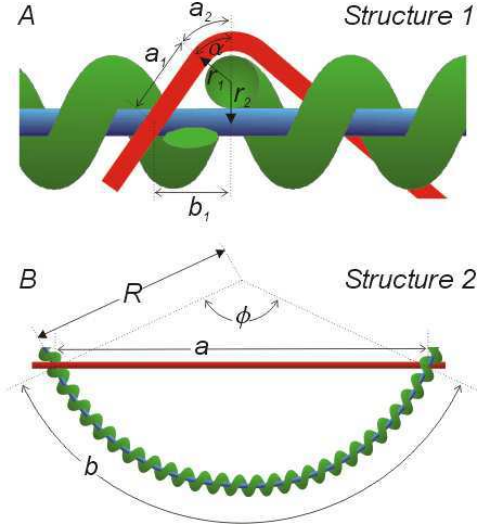


FIG. 5: Two homologous alignments between the same substrates. Red curve = dsDNA molecule (\mathcal{D}); blue line = ssDNA, green helix = RecA filament (\mathcal{R}). (A) Structure 1 (small N). The helix is cut to allow clearer labeling of the figure. The red and blue curves form the double hit loop. The RecA filament (green) passes through this once. Because \mathcal{R} is much stiffer than \mathcal{D} , we assume \mathcal{R} does not bend significantly on this length scale. (B) Structure 2 (large N). Now the RecA filament passes through the double hit loop many times. Because \mathcal{R} is longer here, we include bending with a radius of curvature R . We ignore the bending of \mathcal{D} necessary to enter the RecA filament.

second region is distinct if the RecA filament passes through the double hit loop at least once, otherwise it only extends the first region. We estimate the minimum work to form a double hit loop for different N and show that the resulting Boltzmann factor is too small to permit the structure to form.

When the RecA filament passes through the double hit loop $M = 1$ times we consider N small. This forms *structure 1*, shown in figure 5A. As \mathcal{R} is very stiff it will behave as a rigid rod for small N , so we ignore any bending of \mathcal{R} . To align the N^{th} base(pair) of \mathcal{D} and \mathcal{R} then requires stretching and bending \mathcal{D} . We ignore the work necessary to bend \mathcal{D} and consider only the work needed to stretch it. This underestimates the work, producing a lower bound.

The minimum work $W^*(\eta_{\mathcal{R}})$ required to form

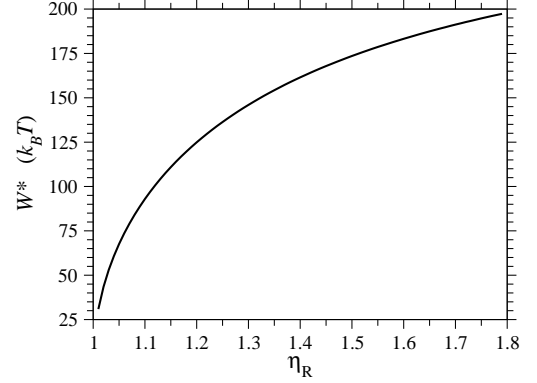


FIG. 6: The minimum work W^* required to form structure 1 as a function of the stretching factor $\eta_{\mathcal{R}}$ of the DNA within substrate \mathcal{R} relative to B-form DNA.

as a function of the stretching factor $\eta_{\mathcal{R}}$ in figure 6. W^* increases with $\eta_{\mathcal{R}}$, making structure 1 more difficult to form. For RecA, $\eta_{\mathcal{R}} = 1.5$ and the work is minimized by $\alpha^* = .84$ and $N^* \approx 25$. We call this the *minimal structure 1*. The energy of this is about $W^* \approx 170k_B T$. The Boltzmann factor is $e^{-E_i/k_B T}$, so the probability of forming structure 1 is on the order of e^{-170} . Formation of a second homologous alignment therefore does not occur for small N as a result of thermal fluctuations.

When the RecA filament passes through the double hit loop $M \geq 2$ times we must include the bending of \mathcal{R} , but we ignore the bending of \mathcal{D} as it enters or leaves the RecA filament. This shortens the path for \mathcal{D} and lengthens the radius of curvature for \mathcal{R} , both of which reduce the work, giving a lower limit on the work required to achieve the second alignment. This is *structure 2*, shown in figure 5B. The minimum work W^* to form structure 2 is calculated in Appendix B.

If $30 \lesssim N \lesssim 100$, the expression for W^* is complicated by the division of the parameter space into different regions. Figures 7A and B are more informative. Figure 7A shows $W^*(N)$ with the persistence length of \mathcal{D} fixed at the biological value of

$\xi_{\mathcal{R}} = 860\text{nm}$ for various values of $\eta_{\mathcal{R}}$. The curves all have a similar shape, with the amplitudes increasing with increasing $\eta_{\mathcal{R}}$. For small N , the minimal structure involves stretching \mathcal{D} without significantly bending \mathcal{R} . In this case,

$$W^* \approx F_0 a_0 (\eta_{\mathcal{D}} - 1) N = F_0 a_0 (\eta_{\mathcal{R}} - 1) N \quad (5)$$

where F_0 is a known constant. Consequently, the left edges of these curves in figure 7A are spaced linearly in proportion to $\eta_{\mathcal{R}}$. For the physiological value of $\eta_{\mathcal{R}} = 1.5$, the minimal structure at first involves only stretching \mathcal{D} and W^* forms a straight line which increases with N as in equation 5. This is because the larger N is, the more base pairs in \mathcal{D} must be stretched. As N increases, the length of the segment of \mathcal{R} between regions 1 and 2 increases and the work required to bend \mathcal{R} decreases. At $N \simeq 48$, it becomes comparable to the work required to stretch \mathcal{D} and the minimal structure becomes a combination of bending \mathcal{R} and stretching \mathcal{D} . As N increases further, the work to bend \mathcal{R} drops further while the work to stretch \mathcal{D} continues to increase so bending \mathcal{R} becomes a steadily larger part of the process. W^* curves downward as this happens, and by $N \simeq 60$ the minimal structure involves only bending \mathcal{R} and no stretching \mathcal{D} . From here on, W^* decreases when N increases as $W^* \propto N^{-2}$.

The location of the transition from the stretching \mathcal{D} regime with $W^* \propto N$ to the bending \mathcal{R} regime with $W^* \propto N^{-2}$ is influenced by $\eta_{\mathcal{R}}$. For larger $\eta_{\mathcal{R}}$, greater work is required to sufficiently stretch a given number of base pairs, making W^* larger for larger values of $\eta_{\mathcal{R}}$. The work required to stretch \mathcal{D} thus becomes comparable to the work required to bend \mathcal{R} at smaller values of N , and the peak value of W^* occurs at smaller N for larger values of $\eta_{\mathcal{R}}$.

Figure 7B shows $W^*(N)$, with $\eta_{\mathcal{R}}$ fixed at the physiological value of $\eta_{\mathcal{R}} = 1.5$, for various values of $\xi_{\mathcal{R}}$. The notable points here are that increasing $\xi_{\mathcal{R}}$ makes it more difficult to bend \mathcal{R} , and therefore W^* increases as $\xi_{\mathcal{R}}$ increases. This also means that higher values of $\xi_{\mathcal{R}}$ push the transition from the stretching \mathcal{D} regime to the bending \mathcal{R} regime to higher values of N . For $\xi_{\mathcal{R}} = 500\text{nm}$ the transition occurs at values of N which are off the left side of figure 7B.

From these figures and from the calculation we see that for $N \lesssim 100$, W^* remains too high for structure 2 to form as a result of thermal fluctuations. This is only the case because of the large values of $\xi_{\mathcal{R}}$ and $\eta_{\mathcal{R}}$, since smaller values of either or both of these decrease W^* and make the structure more accessible to random thermal processes. Since our calculation has produced only a lower limit on W^* we can be confident that this conclusion is valid for values of N which are at least this large.

For $N \gtrsim 60$, the minimal structure is dominated by bending \mathcal{R} , and we can ignore stretching of \mathcal{D} . By contrast, we can no longer ignore the work required to bend \mathcal{D} and \mathcal{R} in the initial alignment phase.

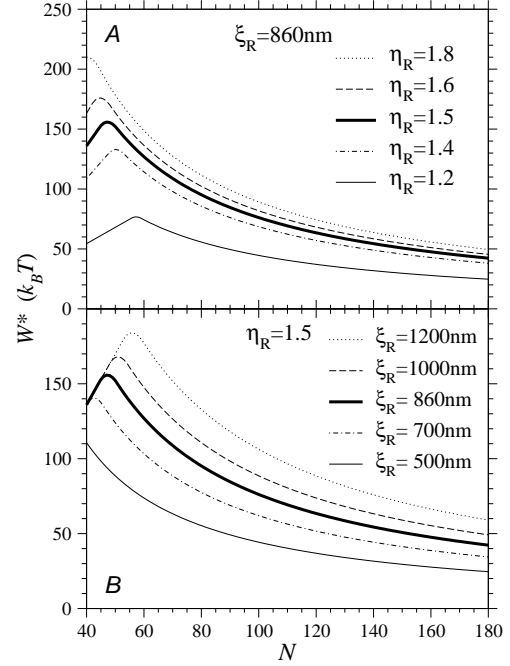


FIG. 7: W^* as a function of N . (A) For various stretching factors $\eta_{\mathcal{R}}$ with the physiological persistence length of $\xi_{\mathcal{R}} = 860\text{nm}$. The thick curve shows the physiological case $\eta_{\mathcal{R}} = 1.5$. (B) For various persistence lengths $\xi_{\mathcal{R}}$ with the physiological stretching factor of $\eta_{\mathcal{R}} = 1.5$. The thick curve shows the physiological case $\xi_{\mathcal{R}} = 860\text{nm}$.

tive force which initially brought them into alignment. This work will be proportional to the length of the substrates between regions one and two. We use ε for the constant of proportionality. The work to form structure 2 in this case is calculated in appendix B. The function is found to have a minimum with respect to N at

$$N^* = \frac{2}{a_0 \eta_{\mathcal{R}}} \sqrt{\left(\frac{\xi_{\mathcal{R}}}{\varepsilon}\right) \left(5 - \sqrt{\frac{30}{\eta_{\mathcal{R}}} - 5}\right)} + 1 \quad (6)$$

This value for N produces the minimal structure 2 for large N . The behavior of N^* in equation 6 with respect to $\eta_{\mathcal{R}}$, as shown in figure 8. N^* has a maximum with respect to $\eta_{\mathcal{R}}$. This occurs at some value $\eta_{\mathcal{R}}^*$ which is found in the appendix to be $\eta_{\mathcal{R}}^* \simeq 1.58$, strikingly close to the physiological value of $\eta_{\mathcal{R}} = 1.5$. This value maximizes the distance between the first and second regions for which the work required to form structure 2 is minimized. Upon using N^* in the expression for work gives the

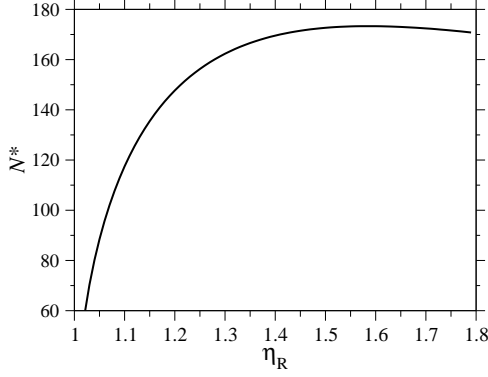


FIG. 8: N^* , the value of N at which the energy required to form structure 2 is minimized, as a function of the stretching factor $\eta_{\mathcal{R}}$. Note that N^* has a maximum with respect to $\eta_{\mathcal{R}}$ at $\eta_{\mathcal{R}} \simeq 1.58$, very near the physiological value of $\eta_{\mathcal{R}} \simeq 1.5$.

$$W^* = 4k_B T \sqrt{(\xi_{\mathcal{R}} \varepsilon) \left(5 - \sqrt{\frac{30}{\eta_{\mathcal{R}}} - 5} \right)}, \quad (7)$$

shown in figure 9. The work W^* increases as the square root of ε . For the physiological values of $\eta_{\mathcal{R}}$ and $\xi_{\mathcal{R}}$, W^* already reaches $\sim 50k_B T$ by $\varepsilon \simeq 0.2\text{nm}^{-1}$, so structure 2 will not form as a result of thermal motions for the physiological values of $\eta_{\mathcal{R}}$ and $\xi_{\mathcal{R}}$ when $\varepsilon \gtrsim 0.2\text{nm}^{-1}$. W^* also increases as the square root of $\xi_{\mathcal{R}}$, and increases with $\eta_{\mathcal{R}}$ in a more complicated fashion. Sufficiently small values of $\eta_{\mathcal{R}}$ or $\xi_{\mathcal{R}}$ would produce values of W^* which would be more accessible to thermal energies.

The probability that a second, local region of homology aligns N base pairs away is $\propto N^{-6}$. This small probability forms an “entropic” barrier to formation of a second region of homology. However, since $\eta_{\mathcal{R}} \simeq \eta_{\mathcal{R}}^*$, the value of N for which the energetic obstacle to alignment is smallest, N^* , is made as large as possible, maximizing the entropic obstacle to alignment. The two processes are “tuned” to work in a complementary fashion, providing a further form of facilitation of the recombination process.

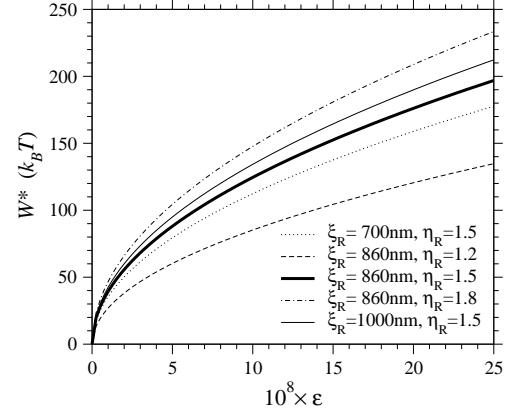


FIG. 9: The minimum work W^* to form structure 2 for $N > 60$ as a function of the constant of proportionality ε for various stretching factors $\eta_{\mathcal{R}}$ and persistence lengths $\xi_{\mathcal{R}}$. The thick curve shows the physiological case $\eta_{\mathcal{R}} = 1.5$ and $\xi_{\mathcal{R}} = 860\text{nm}$.

of stretching of the DNA by the RecA filament and, specifically, to a value close to the physiological value of $\eta_{\mathcal{R}} = 1.5$.

SUMMARY AND CONCLUSION

RecA facilitated homologous recombination derives two advantages from the stiff extended filament and the stretching of the DNA within the filament.

The first is a great increase in the efficiency of the homology search and recognition process. This is a consequence of the increase in σ , the target size for homologous alignment between the substrates. For a region of homology J bases in length stretched by a factor $\eta_{\mathcal{R}}$ we have

$$\sigma = [(J - 1)(\eta_{\mathcal{R}} - 1) + 1] a_0 \quad (8)$$

where a_0 is the spacing of B form DNA. For $\eta_{\mathcal{R}} \simeq 3/2$ this is $\sigma = (J + 1)a_0/2$. This huge σ allows large segments of the substrates to be checked for homology without the need for sliding.

The second advantage is the prevention of topological entanglements. Molecular biological experiments

strand exchange are kept in close proximity by the region of hybrid DNA being formed. This greatly enhances the probability that they will contact each other at additional points. Without the stretching of the DNA within the extended filament, these secondary contacts would often be in homologous alignment and capable of initiating a second homologous strand exchange reaction. This would lead to a trapped state in which a region of counter-wound DNA is trapped between two regions of hybrid DNA, preventing completion of the exchange reaction.

The extended filament prevents homologous alignment at secondary contacts. Homologously aligned secondary contacts can only form through some combination of stretching the DNA external to the filament and bending the filament itself. For moderate distances from the point at which homologous exchange is occurring, thermal fluctuations are incapable of sufficiently bending or stretching the filament for a second hit to occur. For larger distances, thermal fluctuations are also unlikely to separate the locally aligned strands held together by nonspecific electrostatic forces. The interplay between stiffness of the filament and the stretching of the DNA within it ensures that homologous strand exchange between two substrate molecules is initiated at only one point.

Both the stiffness of the filament and the extension of the DNA within it are necessary features of the recombination apparatus. Without them, locating and aligning regions of homology between two DNA molecules would be a slow and inefficient process, and the exchange reaction would be prone to topological traps which would prevent completion of the reaction and resolution of the products. These effects provide a selection pressure to preserve the extended filament as a feature of homologous DNA recombination facilitated by RecA and its homologues.

KK and TC acknowledge support from the National Science Foundation through grant DMS-0206733. KK and RB acknowledge support from the UCLA Dean's Funds.

APPENDIX A: KINETIC PERFECTION IN THE HOMOLOGY SEARCH

Consider \mathcal{D} and \mathcal{R} as defined in the text. The center to center base(pair) spacing is a_0 in \mathcal{D} and $\eta_{\mathcal{R}}a_0$ in \mathcal{R} , so an N base pair segment has length

$$L_{\mathcal{D}} = (N - 1) a_0 \quad (\text{A1})$$

$$L_{\mathcal{R}} = (N - 1) \eta_{\mathcal{R}} a_0 \quad (\text{A2})$$

If \mathcal{D} and \mathcal{R} intersect at a point and rotate around this point until parallel, at most one base within \mathcal{R} and a base pair in \mathcal{D} will be homologously aligned. We wish to determine if this parallel orientation produces an alignment.

To define "aligned" we consider only with the lon-

gitudinal direction. When the aligned base and base pair are homologous they are *homologously aligned*.

To quantify this, first note that the center to center distance between consecutive base pairs of \mathcal{D} is a_0 . Let the longitudinal distance between the centers of the k^{th} base pair on \mathcal{D} and the l^{th} base on \mathcal{R} be $\delta_{k,l}$. These are aligned if

$$|\delta_{k,l}| < \frac{a_0}{2} \quad (\text{A3})$$

Denote the positions of initial contact by $x_{\mathcal{D}}$ along \mathcal{D} and by $x_{\mathcal{R}}$ along \mathcal{R} . The parallel orientation is achieved by rotating around $x_{\mathcal{D}}$ and $x_{\mathcal{R}}$, so these completely determine the relative positions of \mathcal{D} and \mathcal{R} once they are parallel. It is sufficient to fix $x_{\mathcal{R}}$ and ask what values of $x_{\mathcal{D}}$ produce a homologous alignment in the parallel orientation. If the position $x_{\mathcal{D}}$ is moved a distance d along \mathcal{D} , \mathcal{D} will be displaced relative to \mathcal{R} by this same distance d in the parallel orientation. The range of $x_{\mathcal{D}}$ which produces a homologous alignment is therefore the same as the range of longitudinal positions of \mathcal{D} relative to \mathcal{R} which will produce such an alignment.

Consider \mathcal{D} and \mathcal{R} as shown in figure 10A. Number the base pairs beginning with 1 at the left most base pair in the region of homology. Here, \mathcal{D} is as far to the left as possible while maintaining a homologous alignment between \mathcal{D} and \mathcal{R} . The alignment is between base and base pair 1, and the center of base pair 1 is $a_0/2$ to the left of the center of base 1. Figure 10B shows an enlarged view of this.

Moving \mathcal{D} to the right by $a_0/2$ gives figure 10C, where the centers of base pair 1 and base 1 are exactly aligned. Moving \mathcal{D} to the right by $(\eta_{\mathcal{R}} - 1) a_0$ then produces figure 10D, in which the centers of base pair 2 and base 2 are exactly aligned. Each displacement of \mathcal{D} to the right by $(\eta_{\mathcal{R}} - 1) a_0$ now increments by 1 the base and base pair whose centers are exactly aligned. Starting with figure 10C and repeating this motion $(J - 1)$ times produces figure 10E, in which the centers of base pair J and base J are exactly aligned. A final movement of \mathcal{D} to the right by $a_0/2$ produces figure 10F, where \mathcal{D} is as far to the right relative to \mathcal{R} as is possible while still maintaining a homologous alignment between them.

The *target size* σ is range of longitudinal positions of \mathcal{D} relative to \mathcal{R} which produces a homologous alignment between them. This is the change in the position of \mathcal{D} in going from figure 10A to figure 10F, which is given in eq. 1. If $\eta_{\mathcal{R}}$ has the known RecA value of $\eta_{\mathcal{R}} = 3/2$ we get $\sigma = (J + 1) a_0/2$, which scales as the length of the region of homology.

From σ we can estimate the reaction rate. With no sliding[Adzuma 1998], diffusion limits the maximum "on rate" k_a for the reaction to the Debye-Smoluchowski rate. Our target is cylindrical, but the magnitude should be reasonably approximated if we substitute the target length for the diameter of

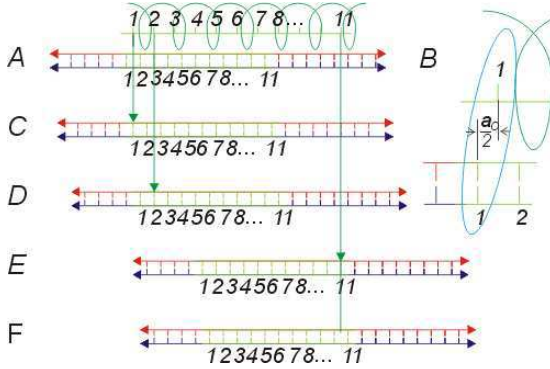


FIG. 10: Dark green helix, RecA filament, light green line inside helix, ssDNA (\mathcal{R}); red and blue lines with light green segments, dsDNA (\mathcal{D}). \mathcal{R} is arbitrarily chosen to be 11 bases in length. The light green region of \mathcal{D} is homologous to \mathcal{R} . (A) \mathcal{D} is as far to the left as possible while maintaining a homologous alignment between \mathcal{D} and \mathcal{R} (between base and base pair 1). (B) Close up of the homologously aligned base and base pair in A. (C) Effect of shifting \mathcal{D} to the right a distance $a_0/2$. (D) Effect of shifting \mathcal{D} further to the right, this time by a distance a_0 . (E) Effect of 9 more consecutive shifts of \mathcal{D} to the right by a distance a_0 . (F) Effect of a final shift of \mathcal{D} to the right by a distance $a_0/2$.

a spherical target, $r \rightarrow \sigma/2$, giving $k_a \simeq 2\pi D_3 \sigma$, where D_3 is the three dimensional diffusion constant. The length of \mathcal{R} is

$$\ell = (J - 1) \eta_{\mathcal{R}} a_0 \simeq J \eta_{\mathcal{R}} a_0 \quad (\text{A4})$$

Upon substituting this for the diameter of a spherical molecule, $r \rightarrow \ell/2$, the three dimensional diffusion constant in a solvent with viscosity η , becomes $D_3 = k_B T / (3\pi \eta \ell)$. Assuming J is reasonably large, $J \eta_{\mathcal{R}} a_0 \gg \ell$, the length of \mathcal{R} is much larger than the diameter of a spherical molecule, $r \rightarrow \ell/2$, giving $k_a \simeq 2\pi D_3 \sigma$.

APPENDIX B: DOUBLE HIT PROBABILITY IN THE RECA RECOMBINATION SYSTEM

If N is small we consider structure 1 as shown in Figure 5A. Define $\eta_{\mathcal{D}}$ and $\eta_{\mathcal{R}}$ as the extension of \mathcal{D} and \mathcal{R} relative to the length of B-form DNA. Let a_0 be the spacing of base pairs in B form DNA and denote the persistence lengths of \mathcal{D} and \mathcal{R} by $\xi_{\mathcal{D}}$ and $\xi_{\mathcal{R}}$ respectively. These have the numerical values $a_0 = 0.34\text{nm}$, $\xi_{\mathcal{D}} \simeq 53\text{nm}$, and $\xi_{\mathcal{R}} \simeq 860\text{nm}$. We model the RecA filament as a cylinder of radius r_{RecA} whose axis follows a helical path of radius $r_2 \simeq 3\text{nm}$. Treating \mathcal{D} as a cylinder of radius $r_{\mathcal{D}}$, the closest approach of the center of \mathcal{D} to the center of \mathcal{R} will be the sum of their radii, which we denote by $r_1 = r_{\text{RecA}} + r_{\mathcal{D}} \simeq 2.5\text{nm}$.

We wish to determine the minimum work required to form structure 1. We ignore bending of \mathcal{R} on this length scale and also ignore the work required to bend \mathcal{D} . We calculate the work solely from the stretching of \mathcal{D} , making our calculation of the work a lower bound.

The angle α can be varied to find the minimal-energy form of structure 1, the form produced with the minimum possible work, subject to two constraints. Steric hinderance between the RecA filament and \mathcal{D} at the points where it enters the RecA filament requires $\alpha \geq \pi/5$, while other physical considerations show that the minimum energy can occur only for $\alpha \leq \pi/2$.

Both regions can simultaneously be in homologous alignment only if N satisfies

$$2(a_1 + a_2) = a_0 \eta_{\mathcal{D}} (N - 1) \quad (\text{B1})$$

$$2b_1 = a_0 \eta_{\mathcal{R}} (N - 1).$$

Since $a_2 = r_1 \alpha$, trigonometry demands

$$a_1 = \frac{r_1 \cos \alpha + r_2}{\sin \alpha} \quad \text{and} \quad b_1 = \frac{r_2}{\tan \alpha} + \frac{r_1}{\sin \alpha} \quad (\text{B2})$$

Using equations B1 and B2 we find

$$(N - 1) = \frac{2}{a_0 \eta_{\mathcal{R}}} \left(\frac{r_1 + r_2 \cos \alpha}{\sin \alpha} \right) \quad (\text{B3})$$

$$\eta_{\mathcal{D}} = \frac{\eta_{\mathcal{R}} (r_1 \alpha \sin(\alpha) + r_1 \cos(\alpha) + r_2)}{r_1 + r_2 \cos \alpha}$$

We make the simplification of assuming that the force to stretch a dsDNA is

$$F_{\mathcal{D}} = \begin{cases} 0 & \text{for } \eta_{\mathcal{D}} < 1 \\ F_0 & \text{for } \eta_{\mathcal{D}} \geq 1 \end{cases} \quad (\text{B4})$$

Here, $F_0 \approx 20k_B T/\text{nm}$, but we leave this parameter free for the present.

Above $\eta_{\mathcal{D}} \approx 1.8$ equation B4 is not valid. Here, the dsDNA is stretched to its maximum length, and the force to stretch it is zero.

it rises rapidly. Further stretching breaks the sugar phosphate backbones of the DNA strands. While our calculation may produce values of $\eta_{\mathcal{D}} > 1.8$, we are not concerned. We only wish to show that the minimal form of structure 1 does not form as a result of random thermal fluctuations, and our calculation will still accomplish this.

Using equation B4 for $F_{\mathcal{D}}$, the work required to stretch the dsDNA to a final extension $\eta_{\mathcal{D}}$ (in units

of $k_B T$) is

$$W_{\mathcal{D}} = \begin{cases} 0 & \text{for } \eta_{\mathcal{D}} < 1 \\ F_0 (\eta_{\mathcal{D}} - 1) a_0 (N - 1) & \text{for } \eta_{\mathcal{D}} \geq 1 \end{cases}$$

Under our approximations, this is the only contribution to the total work. Using equations B3 W becomes a function of the single variable α

$$W(\alpha) = \begin{cases} 0 & \text{for } \eta_{\mathcal{D}} < 1 \\ \frac{2F_0 \csc \alpha}{\eta_{\mathcal{R}}} (-r_1 + r_2 \eta_{\mathcal{R}} + (r_1 \eta_{\mathcal{R}} - r_2) \cos \alpha + r_1 \alpha \eta_{\mathcal{R}} \sin \alpha) & \text{for } \eta_{\mathcal{D}} \geq 1 \end{cases} \quad (\text{B5})$$

Minimizing this with respect to α we find $\alpha^* = \text{arcsec}(\eta_{\mathcal{R}})$ which gives us the equations

$$\begin{aligned} W^* &= 2F_0 \left(r_2 \sqrt{1 - \frac{1}{\eta_{\mathcal{R}}^2}} + r_1 \text{arcsec}(\eta_{\mathcal{R}}) \right) \\ \eta_{\mathcal{D}}^* &= \frac{\eta_{\mathcal{R}} (r_1 + r_2 \eta_{\mathcal{R}} + r_1 \sqrt{\eta_{\mathcal{R}}^2 - 1} \text{arcsec}(\eta_{\mathcal{R}}))}{(r_1 \eta_{\mathcal{R}} + r_2)} \\ N^* &= \frac{2}{a_0} \left(\frac{r_1 \eta_{\mathcal{R}} + r_2}{\eta_{\mathcal{R}} \sqrt{(\eta_{\mathcal{R}})^2 - 1}} \right) + 1 \end{aligned} \quad (\text{B6})$$

With the known values of the constants, equation B6 becomes

$$W^*(\eta_{\mathcal{R}}) = 24k_B T \sqrt{1 - \frac{1}{\eta_{\mathcal{R}}^2}} + 20k_B T \text{arcsec}(\eta_{\mathcal{R}}), \quad (\text{B7})$$

which is plotted in figure 6. At the physiological value of $\eta_{\mathcal{R}} = 3/2$ for the RecA system, $\alpha^* = 0.84$, $\eta_{\mathcal{D}}^* = 2.1$, $N^* = 25$, and $W^* = 174k_B T$. The probability of the system being in the minimal form of structure 1 is on the order of e^{-174} . This vanishing probability persists for $\eta_{\mathcal{D}} = \eta_{\mathcal{D}}^* \simeq 1.8$.

For somewhat larger N we consider structure 2 as shown in figure 5B. The angle α no longer enters the calculation directly, and we deal with the angle ϕ . The parameters are subject to the restrictions $1 \leq \eta_{\mathcal{R}} \leq 1.8$, $\eta_{\mathcal{D}} \leq \eta_{\mathcal{R}}$, and $\xi_{\mathcal{D}} \leq \xi_{\mathcal{R}}$.

The exchange regions can simultaneously be in homologous alignment if N satisfies

$$a = a_0 \eta_{\mathcal{D}} (N - 1) \quad \text{and} \quad b = a_0 \eta_{\mathcal{R}} (N - 1), \quad (\text{B8})$$

from which we find $\eta_{\mathcal{D}}/\eta_{\mathcal{R}} = a/b$.

The radius of curvature R for structure \mathcal{R} is related to the opening angle ϕ by

while trigonometry gives

$$a = 2R \sin\left(\frac{\phi}{2}\right) \quad (\text{B10})$$

Upon using the above,

$$\eta_{\mathcal{D}} = \frac{2\eta_{\mathcal{R}} \sin\left(\frac{\phi}{2}\right)}{\phi} \quad (\text{B11})$$

Using equations B8 and B9 we also find

$$R = \frac{a_0 \eta_{\mathcal{R}} (N - 1)}{\phi} \quad (\text{B12})$$

We can now calculate the work required to form structure 2. We will vary N and ϕ to minimize this. We can then vary $\eta_{\mathcal{R}}$ and $\xi_{\mathcal{R}}$ (subject to $\eta_{\mathcal{R}} \geq \eta_{\mathcal{D}}$ and $\xi_{\mathcal{R}} \geq \xi_{\mathcal{D}}$) to examine their effects on the system. The work to form structure 2 comes from three terms: stretching \mathcal{D} , bending \mathcal{R} , and separating \mathcal{D} from \mathcal{R} against the non-specific attractive force by which they were initially aligned.

The force required to stretch \mathcal{D} to $\eta_{\mathcal{D}}$ times its B-form contour length is approximately

$$F_{\mathcal{D}} = \begin{cases} 0 & \text{for } \eta_{\mathcal{D}} < 1.0 \\ F_0 & \text{for } 1.0 \leq \eta_{\mathcal{D}} \leq 1.8 \\ \infty & \text{for } 1.8 \leq \eta_{\mathcal{D}} \end{cases} \quad (\text{B13})$$

Since $\eta_{\mathcal{D}} \geq 1.8$ is unphysical we impose $F_{\mathcal{D}}(\eta_{\mathcal{D}} \geq 1.8) = \infty$ to ensure that this does not occur. The work to stretch \mathcal{D} is thus

$$W_{\mathcal{D}} = \begin{cases} 0 & \text{for } \eta_{\mathcal{D}} < 1 \\ F_0 (\eta_{\mathcal{D}} - 1) a_0 (N - 1) & \text{for } 1 \leq \eta_{\mathcal{D}} \leq 1.8 \\ \infty & \text{for } 1.8 \leq \eta_{\mathcal{D}} \end{cases} \quad (\text{B14})$$

Using equation B11 and expressing the regime boundaries in terms of ϕ this becomes (in units of

$$W_{\mathcal{D}} = \begin{cases} 0 & \text{for } \left(\frac{\sin(\frac{\phi}{2})}{\frac{\phi}{2}}\right) \eta_{\mathcal{R}} < 1 \\ F_0 \left(\left(\frac{\sin(\frac{\phi}{2})}{\frac{\phi}{2}}\right) \eta_{\mathcal{R}} - 1 \right) a_0 (N-1) & \text{for } 1 \leq \eta_{\mathcal{R}} \left(\frac{\sin(\frac{\phi}{2})}{\frac{\phi}{2}}\right) \leq 1.8 \\ \infty & \text{for } 1.8 < \eta_{\mathcal{R}} \left(\frac{\sin(\frac{\phi}{2})}{\frac{\phi}{2}}\right) \end{cases} \quad (\text{B15})$$

The work to bend \mathcal{R} into the circular arc in structure 2 is

$$W_{\mathcal{R}} = \frac{1}{2} \kappa_{\mathcal{R}} \int \left(\frac{1}{R(s)} \right)^2 ds = \frac{1}{2} \kappa_{\mathcal{R}} \left(\frac{1}{R} \right)^2 b \quad (\text{B16})$$

Using equations B9 and B12 and the fact that $\kappa_{\mathcal{R}} \simeq \xi_{\mathcal{R}}$ (in units of $k_B T$), gives

$$W_{\mathcal{R}} = \frac{\xi_{\mathcal{R}}}{2} \left(\frac{\phi^2}{a_0 \eta_{\mathcal{R}} (N-1)} \right) \quad (\text{B17})$$

There is a non-specific attractive interaction between \mathcal{D} and \mathcal{R} . The work to pull \mathcal{D} and \mathcal{R} apart is approximately proportional to the length of \mathcal{R}

between the exchange regions. For intermediate N we ignore an energetic contribution $\propto \varepsilon k_B T a_0 \eta_{\mathcal{R}} N$, which underestimates the work and produces a lower bound,

$$W(\phi) = \begin{cases} W_{\mathcal{R}} & \text{for } \left(\frac{\sin(\frac{\phi}{2})}{\frac{\phi}{2}}\right) \eta_{\mathcal{R}} < 1 \\ W_{\mathcal{D}} + W_{\mathcal{R}} & \text{for } 1 \leq \eta_{\mathcal{R}} \left(\frac{\sin(\frac{\phi}{2})}{\frac{\phi}{2}}\right) \leq 1.8 \\ \infty & \text{for } 1.8 < \eta_{\mathcal{R}} \left(\frac{\sin(\frac{\phi}{2})}{\frac{\phi}{2}}\right) \end{cases} \quad (\text{B18})$$

Upon minimizing the work $W(\phi)$ with respect to the angle ϕ , we find ϕ^* and

$$W(\phi^*) \equiv W^* = a_0 F_0 (N-1) \eta_{\mathcal{R}} \left\{ \left(\frac{\eta_{\mathcal{R}} - 1}{\eta_{\mathcal{R}}} \right) + \left(\frac{1}{120} \max \left[0, \min \left[10 - 2\sqrt{\frac{30}{\eta_{\mathcal{R}}}} - 5, 10 - \frac{120 k_B T \xi_{\mathcal{R}}}{a_0^2 F_0 (N-1)^2 \eta_{\mathcal{R}}^2} \right] \right] \right) \right\} \\ \times \left(\frac{240 k_B T \xi_{\mathcal{R}}}{a_0^2 F_0 (N-1)^2 \eta_{\mathcal{R}}^2} - 20 \max \left[0, \min \left[10 - 2\sqrt{\frac{30}{\eta_{\mathcal{R}}}} - 5, 10 - \frac{120 k_B T \xi_{\mathcal{R}}}{a_0^2 F_0 (N-1)^2 \eta_{\mathcal{R}}^2} \right] \right] \right) \quad (\text{B19})$$

This function is plotted in figures 7A and B using standard values for a_0, F_0 , and $k_B T$. From figures 7A and B it is clear that by $N \approx 60$ the minimal form of structure 2 is dominated by bending \mathcal{R} . For large N , ($\gtrsim 60$), the interaction energy can no longer be ignored, but now we always have $\left(\frac{\sin(\frac{\phi}{2})}{\frac{\phi}{2}}\right) \eta_{\mathcal{R}} < 1$. The total work thus simplifies to

$$W = \frac{4k_B T \left(5 - \sqrt{\frac{30}{\eta_{\mathcal{R}}} - 5} \right) \xi_{\mathcal{R}}}{a_0 (N-1) \eta_{\mathcal{R}}} + \varepsilon k_B T a_0 \eta_{\mathcal{R}} (N-1) \quad (\text{B20})$$

The separation between exchange regions which minimizes this and the corresponding minimum

work are

$$N^* = \frac{2}{a_0 \eta_{\mathcal{R}}} \sqrt{\left(\frac{\xi_{\mathcal{R}}}{\varepsilon} \right) \left(5 - \sqrt{\frac{30}{\eta_{\mathcal{R}}} - 5} \right)} \quad (\text{B21})$$

and

$$W^* = 4k_B T \sqrt{(\xi_{\mathcal{R}} \varepsilon) \left(5 - \sqrt{\frac{30}{\eta_{\mathcal{R}}} - 5} \right)}. \quad (\text{B22})$$

These are plotted in figures 8 and 9 respectively. We also note that N^* is monotonic with respect to the $\xi_{\mathcal{R}}$ and ε but has a maximum with respect to $\eta_{\mathcal{R}}$ at $\eta_{\mathcal{R}}^* = \frac{5}{4} (3 + \sqrt{3}) \simeq 1.58$.

- Bustamante. 1999. *Proc. Natl. Acad. Sci. USA*. 96:10109-10114.
- [Heuser & Griffith 1989] Heuser, J., and J. Griffith. 1989. *J. Mol. Biol.* 210:473-484.
- [Honigberg & Radding 1998] Honigberg, S., and C. Radding. 1998. *Cell*. 54:525-532.
- [Karlin & Brocchieri 1996] Karlin, S., and L. Brocchieri. 1996. *J. Bacteriology*. 178:1881-1894.
- [Menetski *et al.* 1990] Menetski, J. P., D. G. Bear, and S. C. Kowalczykowski. 1990. *Proc. Natl. Acad. Sci. USA*. 87:21-25.
- [Nishinaka *et al.* 1997] Nishinaka, T., Y. Ito, S. Yokoyama, and T. Shibata. 1997. *Proc. Natl. Acad. Sci. USA*. 94:6623-6628.
- [Nishinaka *et al.* 1998] Nishinaka, T., A. Shinohara, Y. Ito, S. Yokoyama, and T. Shibata. 1998. *Proc. Natl. Acad. Sci. USA*. 95:11071-11076.
- [Roca & Cox 1997] Roca, A. I., and M. M. Cox. 1997. *Prog. Nucleic Acids Res. Mol. Biol.* 56:129-223.
- [Rosselli & Stasiak 1990] Rosselli, W., and A. Stasiak. 1990. *J. Mol. Biol.* 216:335-352.
- [Takahashi & Norden 1994] Takahashi, M., and B. Norden. 1994. *Adv. Biophys.* 30:1-35.
- [White *et al.* 1988] White, J. H., N. R. Cozzarelli, and W. R. Bauer. 1988. *Science*. 241:323-327.
- [Yu & Egelman 1992] Yu, X., and E. H. Egelman. 1992. *J. Mol. Biol.* 227:334-346.